Journal of Biomechanics 47 (2014) 137–147

Contents lists available at ScienceDirect

Journal of Biomechanics

journal homepage: www.elsevier.com/locate/jbiomech
www.JBiomech.com

Mechanobiology of low-density lipoprotein transport within an arterial wall—Impact of hyperthermia and coupling effects

Stephen Chung, Kambiz Vafai *

Department of Mechanical Engineering, University of California, Riverside, CA 92521, United States

ARTICLE INFO

Article history:
Accepted 24 September 2013

Keywords:
Low-density lipoprotein transport
Multi-layered arterial wall
Porous media
Hyperthermia
FSI
Osmosis
Soret and Dufour effect

ABSTRACT

The effects of hyperthermia, coupling attributes and property variations on Low-density lipoprotein (LDL) transport within a multi-layered wall while accounting for the fluid structure interaction (FSI) is analyzed in this work. To understand the potential impact of the hyperthermia process, thermo-induced attributes are incorporated, accounting for the plasma flow, mass transfer, as well as the elastic wall structure. The coupling effect of osmotic pressure, Soret and Dufour diffusion is discussed and their influence on LDL transport is examined, demonstrating that only the Soret effect needs to be accounted for. The effect of thermal expansion on changing the behavior of flow, mass transport, and elastic structure is illustrated and analyzed while incorporating the variations in the effective LDL diffusivity and consumption rate, as well as other dominating parameters. It is shown that hyperthermia results in an enhancement in LDL transport by increasing the concentration levels within the arterial wall.

1. Introduction

Cardiovascular diseases have received considerable attention due to their impact on health issues within the society and 80 million adults patients in America alone (American Heart Association, 2007; Khakpour and Vafai, 2008) with half a trillion dollars in expenses (American Heart Association, 2008; Hossain et al., 2011). Atherosclerosis usually occurs in larger arteries and can lead to other kinds of cardiovascular diseases. This aortic disease is not only associated with 1/5 of deaths in the United States by its complications (American Heart Association, 2008; Hossain et al., 2011) but also the 14th cause of death in America by itself (Gillum, 1995; Khanafer et al., 2009). Studying atherosclerosis is important for a better diagnosis and treatment of this disease.

Low-density lipoprotein (LDL), is considered to be one of the main factors in causing atherosclerosis as it accumulates in an arterial wall. Oxidization of LDL damages the cells and the wall function of an artery, resulting in the plaque formation and lumen stenosis. An accurate and comprehensive model of LDL molecule accumulation in the wall, can demonstrate the involved processes leading to atherosclerosis. Wall-free and lumen-wall models were introduced earlier and have been used by other researchers (Rappitsch and Perktold, 1996; Wada and Karino, 2000; Moore and Ethier, 1997; Stangeby and Ethier, 2002a, b; Prosi et al., 2005). However, the structure and phenomena within the arterial wall is complex as shown in Fig. 1a, and a detailed multi-layered model with different consideration in each of the layers of an artery is far more appropriate. Transport phenomena through porous media has been studied for numerous different fields of research (Tien and Vafai, 1989; Vafai and Hadim, 2000; Razi et al., 2005; Li and Stoliarov, 2013). Darcy and extended Darcy models have been applied in earlier works (Chung and Vafai, 2010; Shi and Vafai, 2010).

Yang and Vafai (2006, 2008) and Ai and Vafai (2006) developed a multi-layered model in an artery to accurately represent different transport behavior within each of the layers. Four arterial layers, endothelium, intima, IEL, and media, were considered. The Staverman–Kedem–Katchalsky membrane equation (Kedem and Katchalsky, 1958) and osmotic pressure were invoked to describe the transport through a thin porous membrane with low permeability. Based on this model, the impact of macro-structure such as stenosis (Ai and Vafai, 2006; Khanafer et al., 2009) or bifurcation (Khakpour and Vafai, 2008) has also been studied. Furthermore, Chung and Vafai (2012, 2013) coupled the model with extended physics to represent the effect by fluid-structure interactions and atherosclerotic plaque.

Characteristics and properties of transport within these layers have been studied, both from macro-scale view point (Huang et al., 1994; Tada and Tarbell, 2004; Prosi et al., 2005; Ai and Vafai, 2006) as well as a micro-scale point of view (Curry, 1984a, b; Fry, 1985; Huang et al., 1992; Hunag et al., 1997; Huang and Tarbell, 1997; Yuan et al., 1991; Weinbaum et al., 1992; Karner et al., 2001; Liu et al., 2011; Chung and Vafai, 2012, 2013). Several theorems have been developed to calculate the properties by the parameters that describe the microstructure in each of the different arterial layers,

* Corresponding author. Tel.: +1 909 787 2135; fax: +1 909 787 2899.
E-mail address: vafai@engr.ucr.edu (K. Vafai).

0021-9290/$ - see front matter © 2013 Elsevier Ltd. All rights reserved.
http://dx.doi.org/10.1016/j.jbiomech.2013.09.030

Nomenclature

c	LDL concentration
c_T	thermal capacity
D	LDL diffusivity
f_s	solid domain body force
k	reaction coefficient
k_T	thermal-diffusion coefficient
k_D	diffusivity effective rate
K	hydraulic permeability
L	length of the artery
M	molecular weight
p	hydraulic pressure
r	radial location from the centerline
r_m	molecular radius
R	universal gas constant
R_0	radius of lumen domain
T	temperature
T_H	hyperthermia temperature applied at the Lunmen-wall interface
T_{ref}	reference temperature chosen as core body temperature (310 K)
u	axial velocity of blood flow
$\vec{u}$	velocity vector
U_0	maximum velocity at entrance
v	filtration (radial) velocity
x	axial location from the inlet
α	thermal diffusivity
α_{lj}	ratio of LDL molecule radius to half-width of the leaky junction
β_{lj}	leaky-bulk expansion ratio
β_T	thermal expansion coefficient
ε	elastic strain
ε_T	thermal strain
μ	viscosity
σ	reflection coefficient
σ_s	Cauchy stress tensor
ΔT	temperature drop from inner to outer surface of the wall

Subscripts

0	refers to entrance condition
70 mmHg	refers to property under 70 mmHg pressure drop across the wall without hyperthermia
eff	refers to effective property
end	refers to endothelium property
f	refers to plasma property
lj	refers to leaky junction property

such as pore theorem and fiber matrix model which have been utilized by Huang et al. (1994), Karner et al. (2001), Liu et al. (2011) and Chung and Vafai (2012, 2013).

Hyperthermia is involved as an important factor or solution in several health issues, such as cancer treatment (Jain, 1987) or vascular stent delivery (Stoeckel et al., 2004), and the application can possibly be extended to treatment of atherosclerosis or other cardiovascular diseases. Therefore, for transport within an artery, since thermal impact is an important issue, the consideration of heat-induced effect is also important. Mass flux driven by temperature gradient (Soret effect) and its counter part Dufour effect need to be analyzed particularly for hyperthermia applications. Furthermore, based on Einstein- Stoke model, the molecular diffusivity is dominated by temperature. The thermal expansion behavior of an artery has been studied by a number of researchers (Rabin and Plitz, 2005; Jimenez Rios and Rabin, 2006), and hyperthermia can change the of transport properties, based on Chung and Vafai (2012) FSI work. Another aspect which can be affected by temperature is the reaction rate of LDL in the media layer.

In summary, the current work aims at investigating the impact of coupling effect between hydraulic, mass, and heat transport, by examining influence of osmotic, Soret, and Dufour effects. Further, to study the impact of the hyperthermia effect on molecular transport in an artery, thermal expansion, as well as temperature-dependent effective diffusivity and reaction rate of LDL, is analyzed. This study provides, for the first time, a detailed understanding of the physics that can potentially be induced by hyperthermia treatment for cardiovascular issue.

2. Formulation

2.1. Multi-layer model

Fig. 1a shows the layered structure of an arterial wall with, from inner to the outer side, lumen, glycocalyx, endothelium, intima, IEL, media, and adventitia layers. Glycocalyx in this study is neglected (Yang and Vafai, 2006, 2008; Ai and Vafai, 2006) due to its negligible resistance (Michel and Curry, 1999; Tarbell, 2003), while adventitia is incorporated as part of the outer boundary condition for flow, heat and mass transfer. A cylindrical geometry is adopted to represent the computational domain with lumen radius of R_0 (310 μm), axial length L (0.2232 m). Detailed information of the other layers surrounding the lumen are given in Table 1a (Karner et al., 2001; Prosi et al., 2005; Yang and Vafai, 2006, 2008; Ai and Vafai, 2006; Khanafer and Berguer, 2009; Chung and Vafai, 2012, 2013). The transport properties of arterial layers are obtained using either pore theorem or fiber matrix model using the micro-structure information (Karner et al., 2001; Chung and Vafai, 2012). The properties in this table are only given by their original value, and can be affected under the impact of thermal or elastic effects.

2.2. Governing equations—Original and uncoupled

Assuming steady state based on the negligible effect of blood pulsation (Yang and Vafai, 2006; Chung and Vafai, 2012), the conservation of mass, momentum and species inside the lumen are expressed as

$$\nabla \cdot \vec{u} = 0 \tag{1}$$

$$-\nabla p + \mu_f \nabla^2 \vec{u} = 0 \tag{2}$$

$$\vec{u} \cdot \nabla c = D_f \nabla^2 c \tag{3}$$

where $\vec{u}$ is the velocity vector, c LDL concentration, p hydraulic pressure, and μ_f and D_f are the plasma viscosity and diffusivity coefficient, respectively.

The Darcy–Brinkman equation is used to describe the flow, while diffusion–convection–reaction equation incorporating the Staverman–Kedem–Katchalsky membrane equation (Kedem and Katchalsky, 1958) is applied to describe molecular transport of LDL

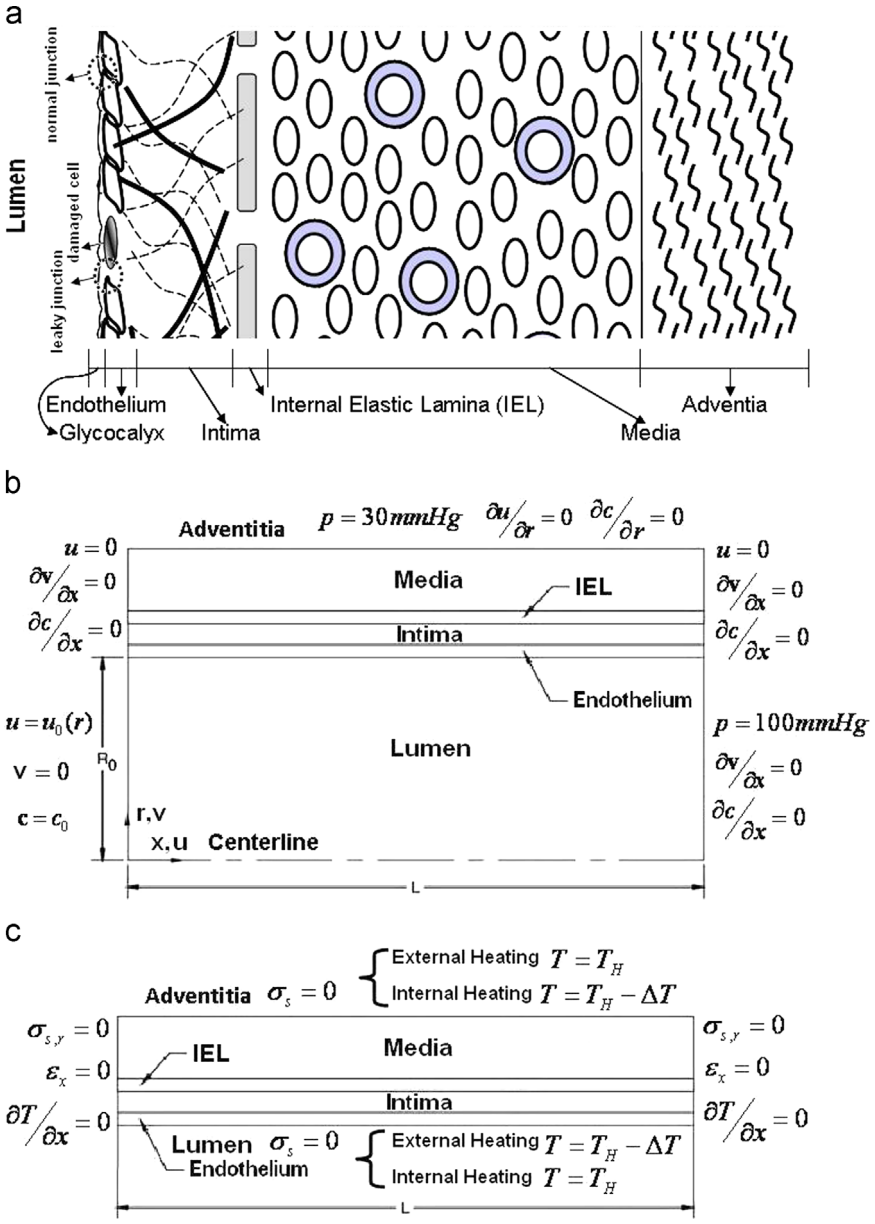

Fig. 1. Configuration for (a) an arterial wall and its layered structure including glycocalyx, endothelium, intima, IEL, media, and adventitia, and analyzed domain and boundary conditions of (b) flow, mass transfer, (c) elastic, and heat transfer models.

Table 1
Transport properties for each of the layers/domains (Chung and Vafai, 2012).

Property	Lumen	Endothelium	Intima	IEL	Media	Adventitia
Thickness $[\mu m]$	**3100**	**2**	**10**	**2**	**200**	**100**
Density ρ $[kg/m^3]$	1.07×10^3	1.057×10^3	1.057×10^3	1.057×10^3	1.057×10^3	–
Viscosity μ_{eff} $[kg/m \cdot s]$	3.7×10^{-3}	0.72×10^{-3}	0.72×10^{-3}	0.72×10^{-3}	0.72×10^{-3}	–
Hydraulic permeability K $[m^2]$	–	3.22×10^{-21} [a]	2×10^{-16}	4.392×10^{-19}	2×10^{-18}	–
LDL effective diffusivity D_{eff} $[m^2/s]$	2.87×10^{-11}	5.7×10^{-18} [a]	5.4×10^{-12}	3.18×10^{-15}	5×10^{-14}	–
Refection coefficient σ	–	0.9888 [a]	0.8272	0.9827	0.8836	–
Reaction coefficient k $[s^{-1}]$	0	0	0	0	3.197×10^{-4}	–
Elasticity $[MPa]$	–	2 [b]	2 [b]	2 [b]	6 [b]	4 [b]
Thermal diffusivity α $[m^2/s]$	–	1.42×10^{-7} [c]	1.42×10^{-7} [c]	1.42×10^{-7} [c]	1.42×10^{-7} [c]	–

The rest of properties are from Yang and Vafai (2006).

[a] The endothelium parameters under $\Delta p$of 70 mmHg are calculated by Chung and Vafai (2012).
[b] The elastic parameters are from Khanafer and Berguer (2009) and Chung and Vafai (2012).
[c] The thermal parameters are from Kolios et al. (1995) and Kotte et al. (1996).

(Yang and Vafai, 2006; Ai and Vafai, 2006, Chung and Vafai, 2012, 2013). Therefore, the flow and mass transfer governing equations are given as

$$\nabla \cdot \vec{u} = 0 \tag{4}$$

$$-\nabla p + \mu_{\text{eff}} \nabla^2 \vec{u} - \frac{\mu_{\text{eff}}}{K} \vec{u} = 0 \tag{5}$$

$$(1-\sigma)\, \vec{u} \cdot \nabla c = \nabla \cdot (D_{\text{eff}} \nabla c) - kc \tag{6}$$

where μ_{eff} is the effective fluid viscosity, K hydraulic permeability; σreflection coefficient; D_{eff} effective LDL diffusivity, k reaction coefficient which is 3.197×10^{-4} $[s^{-1}]$ inside the media layer and zero in the other layers (Prosi et al., 2005; Yang and Vafai, 2006, 2008).

2.3. Governing equations—FSI and hyperthermia

The heat transfer within an arterial wall is described by the energy conservation equation, expressed as

$$\vec{u} \cdot \nabla T = \alpha \nabla^2 c \tag{7}$$

where T is the temperature and α the thermal diffusivity. It should be noted that different porosity and structure within each of the layers does not affect thermal diffusivity much as they do for mass diffusivity. Therefore, the thermal diffusivity is assumed to be uniform (Kolios et al., 1995; Kotte et al., 1996).

The elastic structure of the arterial wall is described by a hyper-elastic model using an elastodynamic equation, described as

$$\nabla \sigma_s + f_s = 0 \tag{8}$$

where f_s is the solid domain body force and σ_s is the Cauchy stress tensor. For strain–stress relationship, Mooney–Rivlin material model is invoked to correlate Cauchy stress tensor σ_s with replacement (Khanafer and Berguer, 2009). Strain due to hydraulic effect is embedded into the properties by assuming that pressure difference through the wall stays constant at 70 mmHg.

2.4. Governing equations—Coupling effect

Osmotic pressure expression is presented by $RT\sigma\nabla c$ where R is the universal gas constant. Similar to osmotic effect, the temperature gradient can also cause the energy potential to drive

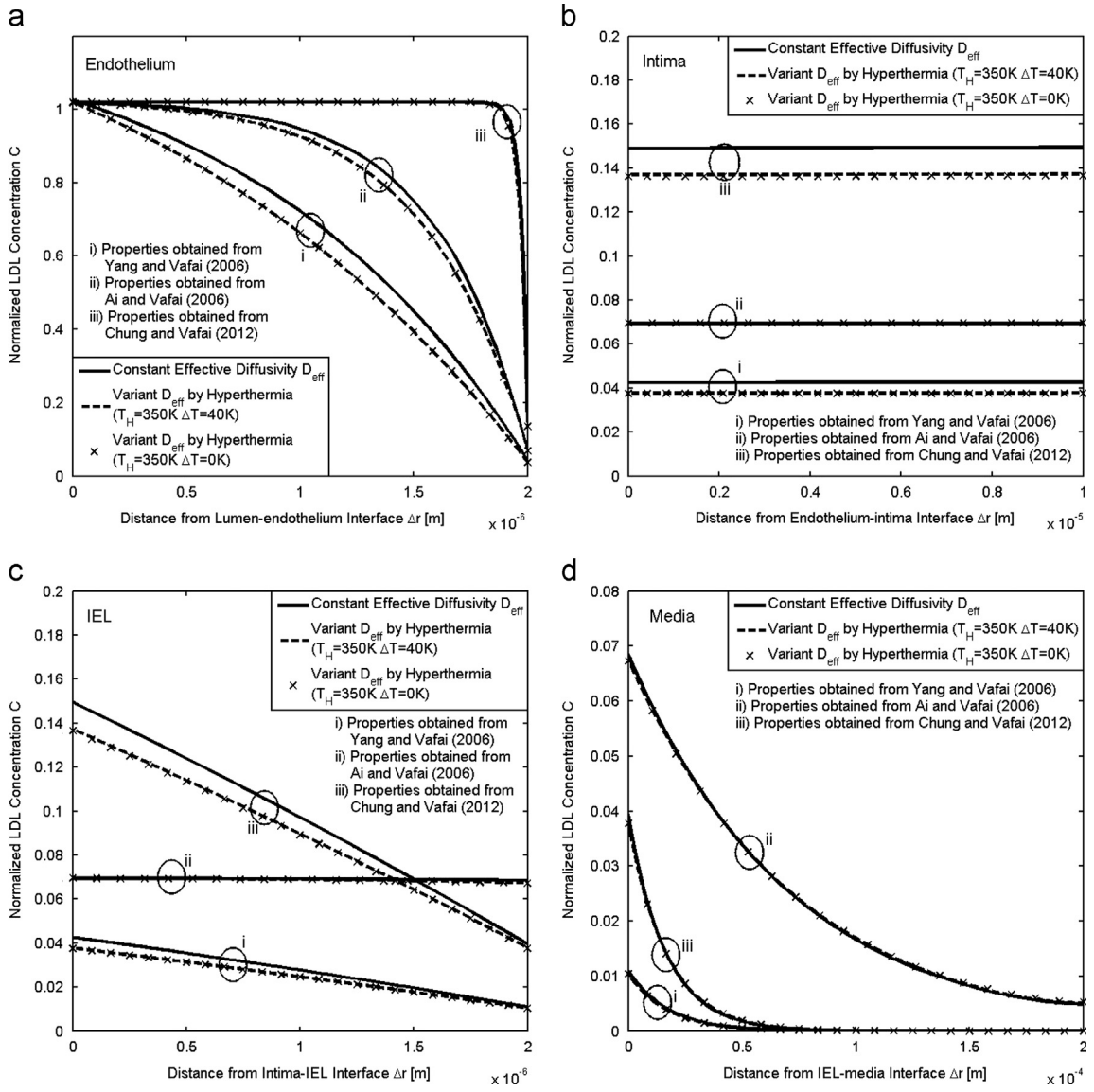

Fig. 2. LDL concentration profile across (a) endothelium, (b) intima, (c) IEL, and d) media, for different set of properties from the works by Yang and Vafai (2006), Ai and Vafai (2006), and Chung and Vafai (2012).

molecular movement from higher to lower temperatures. The Soret diffusion is given by $D_{eff}\frac{k_T\rho_f}{TM_f}\nabla^2 T$ (Chapman and Cowling, 1952; Wakeham et al., 1991; Kays and Crawford, 1993), where k_T is the thermal-diffusion coefficient, M_f the molecular weight of solvent (plasma), and ρ_f is the density of plasma. The counter part of the Soret effect is the Dufour effect, which indicates that the molecular transport will enhance heat transfer by the energy carried by the solute. Dufour effect is represented by $\frac{RTk_T}{c_T M_f c}\nabla\cdot(D_{eff}\nabla c)$ where c_T is the plasma's thermal capacity. Incorporating these three physical effects, the coupling equations for flow, heat and mass transfer can be represented as

$$-\nabla p+\mu_{\text{eff}}\nabla^2\vec{u}-\frac{\mu_{\text{eff}}}{K}\vec{u}+RT\sigma\nabla c=0 \tag{9}$$

$$(1-\sigma)\vec{u}\cdot\nabla c=\nabla\cdot(D_{\text{eff}}\nabla c)+\frac{k_T\rho_f}{TM_f}\nabla\cdot(D_{\text{eff}}\nabla T)-kc \tag{10}$$

$$\vec{u}\cdot\nabla T=\alpha\nabla^2 T+\frac{RTk_T}{c_T M_f c}\nabla\cdot(D_{\text{eff}}\nabla c) \tag{11}$$

2.5. Boundary conditions

The boundary conditions are given in Fig. 1b for momentum, mass transfer, thermal and elastic models. The entrance of lumen is set to have a fully developed entrance velocity $u_0(r)$ expressed by

$$u_0=U_0(1-(r/R_0)^2)\quad at\ \ x=0,\ \ 0\le r\le R_0 \tag{12}$$

with a maximum entrance velocity U_0 of 0.338 m/s (Yang and Vafai, 2006; Karner et al., 2001), and an LDL concentration c_0 of 28.6×10^{-3} mol/m^3 (Katz, 1985; Tarbell, 1993; Yang and Vafai, 2006). Hydraulic pressure p is set with fixed values of 100 $mm\,Hg$ and 30 $mm\,Hg$ on the two sides of the arterial wall (Meyer et al.,

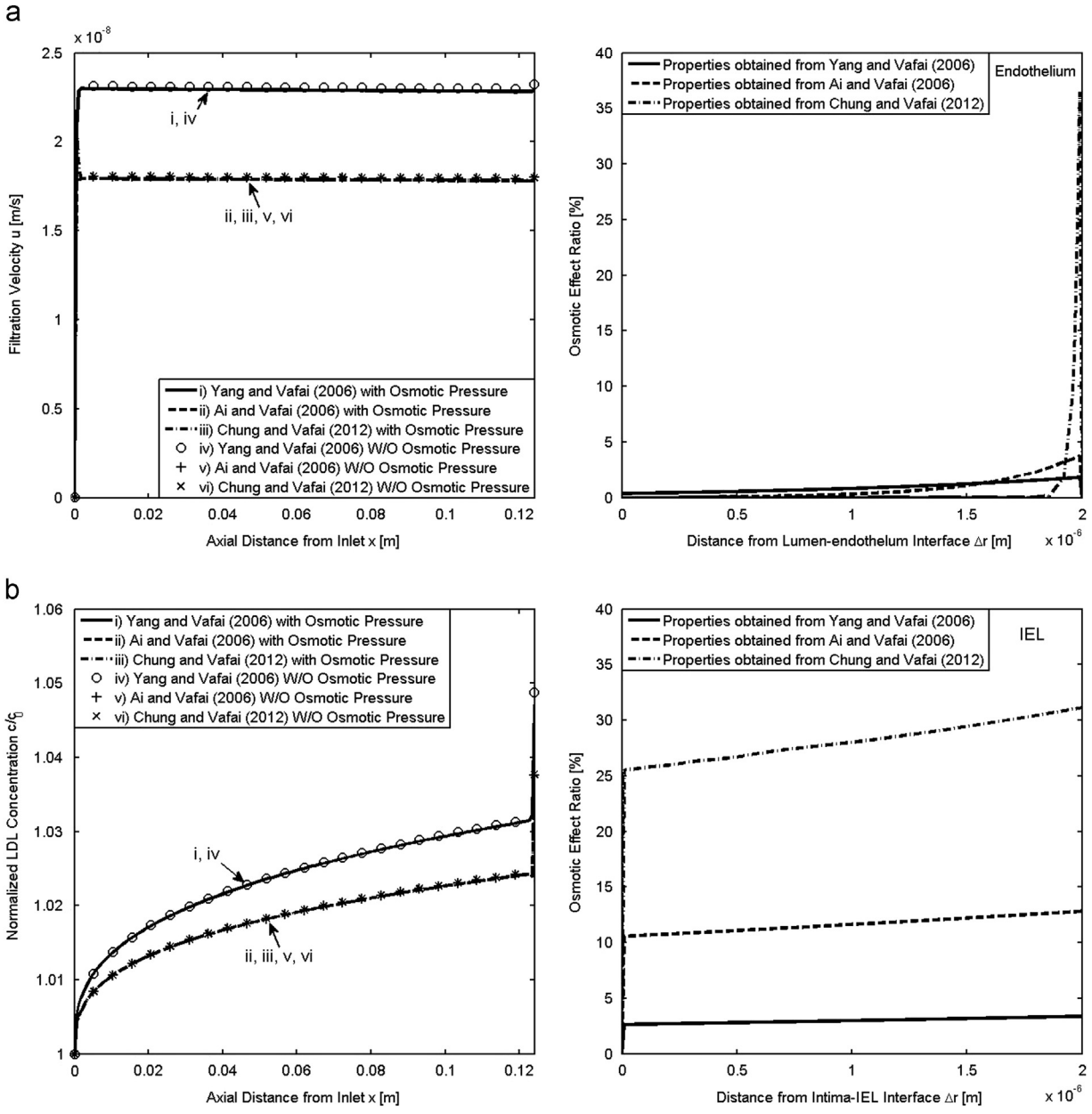

Fig. 3. Effect of different sets of properties and the Osmotic pressure on (a) Filtration velocity and LDL concentration distribution at the lumen-endothelium interface and (b) across endothelium and IEL where highest concentration gradients appears.

1996; Yang and Vafai, 2006). Both internal and external heating by hyperthermia are examined and described by a higher temperature T_H at inner or outer surface of the wall and a lower temperature with temperature drop of ΔT at the other surface as shown in Fig. 1c. Both inner and outer surfaces of arterial wall are set as a free surface since the hydraulic impact is embedded within the transport properties (Chung and Vafai, 2012). Mass continuity condition incorporating the Staverman filtration (Yang and Vafai, 2006; Chung and Vafai, 2012) is expressed as:

$$\left[(1-\sigma)vc - D_{eff}\frac{\partial c}{\partial r}\right]\Big|_{+} = \left[(1-\sigma)vc - D_{eff}\frac{\partial c}{\partial r}\right]|_{-} \quad (13)$$

where v is the filtration velocity of the blood flow penetrating through the arterial wall in the radial direction.

2.6. Pore theorem and thermal expansion

Endothelium causes the most hydraulic and mass transfer resistance across the wall compared to other arterial layers due to its low porosity and small pore size. Therefore, the endothelium pore expansion due to elastic deformation on the arterial wall will have a much higher impact on the flow and mass transfer characteristics within an artery. Based on the work of Chung and Vafai (2012), leaky junctions of endothelium are expanded with a larger cross-sectional area, while normal junctions with smaller cross-section and stronger structure are not affected. The Pore theorem, which is well accepted for calculating transport properties of endothelium (Curry, 1984a, b; Huang et al., 1992; Karner et al., 2001; Chung and Vafai, 2012), is utilized here to couple the thermal expansion.

Transport properties of endothelium given in Table 1 are obtained by Chung and Vafai (2012) based on a 70 mmHg pressure drop across the arterial wall, using the pore theorem with corresponding half-width of the leaky junction of 14.34 nm. On the other hand, the impact of thermal expansion due to hyperthermia is considered through the thermal strain ε and temperature T relationship given by:

$$\varepsilon_T = \beta_T(T - T_{ref}) \quad (14)$$

where β_T is the thermal expansion coefficient with a value of $6.376\times10^{-5}1/K$ (Rabin and Plitz, 2005; Jimenez Rios and Rabin, 2006) and T_{ref} is the reference temperature given as the regular organ temperature of 310 K. The cross-sectional expansion rate of endothelium leaky junction ε_{lj} is calculated from thermal strain ε and leaky-bulk deformation rate β_{lj} (Chung and Vafai, 2012) by

$$\varepsilon_{lj} = \beta_{lj}\varepsilon \quad (15)$$

Applying the pore theorem, the endothelium permeability K_{end} is expressed as:

$$K_{end} = K_{lj} + K_{nj} \quad (16)$$

$$K_{lj} = K_{lj,70\ mmHg}(1+\beta_{lj}\varepsilon)^3 \quad (17)$$

where K_{lj} and K_{nj} are hydraulic permeabilities through leaky and normal junctions.

In this study, the normal junction is assumed to be impermeable for the LDL molecule ($D_{nj}=0;\ \sigma_{nj}=1$), since its radius (5.5 nm) is smaller than the radius of LDL molecule ($r_m=11$ nm). Therefore, using the pore theorem, the effective diffusivity D_{end} and reflection coefficients σ_{end} can be calculated (Chung and Vafai, 2012) as:

$$D_{end} = D_{lj} = D_{lj,70\ mmHg}\frac{k_D}{k_{D,70\ mmHg}} \quad (18)$$

$$k_D = (1-\alpha_{lj})(1-1.004\alpha_{lj}+0.418\alpha_{lj}^3+0.2104\alpha_{lj}^4-0.169\alpha_{lj}^5)/\alpha_{lj} \quad (19)$$

$$\sigma_{end} = 1 - \frac{(1-\sigma_{lj})K_{lj}}{K_{end}} \quad (20)$$

$$\sigma_{lj} = 1-\left(1-\frac{3}{2}\alpha_{lj}^2+\frac{1}{2}\alpha_{lj}^3\right)\left(1-\frac{1}{3}\alpha_{lj}^2\right) \quad (21)$$

$$\alpha_{lj} = \alpha_{lj,70\ mmHg}/(1+\beta_{lj}\varepsilon) \quad (22)$$

where D_{lj} and σ_{lj} are diffusivity and reflection coefficient through the leaky junction, k_D diffusivity effective rate, α_{lj} the ratio of LDL molecule radius to half-width of the leaky junction. $\alpha_{lj,70\ mmHg}$ is obtained as 0.7669 in Chung and Vafai (2012) work, resulting in $k_{\alpha,70\ mmHg}=0.1357$ and $\sigma_{lj,70\ mmHg}=0.7240$.

3. Methodology

The validation for the methodology utilized in the present study is given in the work of Chung and Vafai (2012). Fig. 2 shows comparison of LDL concentration

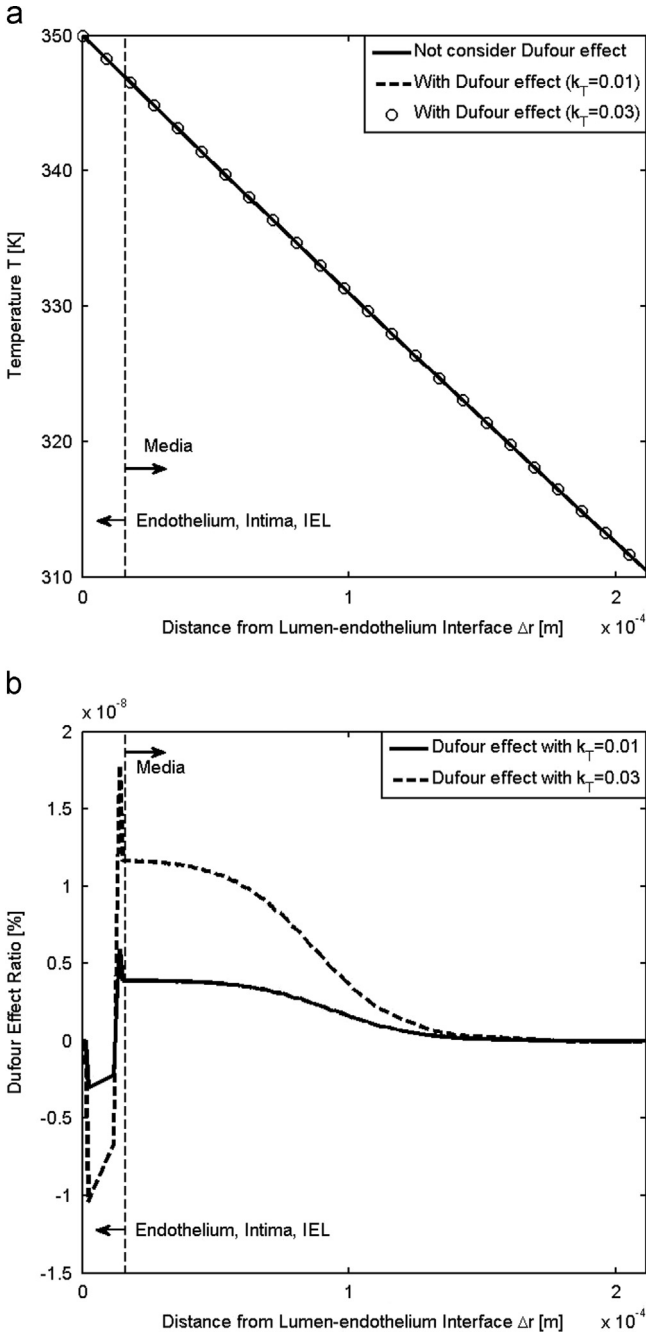

Fig. 4. Dufour effect on (a) temperature distribution within the arterial wall, (b) comparison with ordinary diffusion.

profiles obtained with properties utilized by Yang and Vafai (2006), Ai and Vafai (2006), and Chung and Vafai (2012). The transport properties applied in the three works are obtained by different methods, and result in different LDL concentration distribution especially within endothelium. As such, the main difference in the results between the three methods is characterized by mass transfer Peclet numbers of about 1, 5, and 70 respectively (Yang and Vafai, 2006; Ai and Vafai, 2006; Chung and Vafai, 2012) which represents the competition between diffusive and convective molecular transport. As a result, the concentration gradient driving the penetration in the endothelium can be smooth (Yang and Vafai, 2006), locally enhanced (Chung and Vafai, 2012), or in between (Ai and Vafai, 2006). Fig. 2 also illustrates the effect of variant diffusivity, which will be discussed later. It should be mentioned that in an earlier work of Ai and Vafai (2006), the numerical results were compared with data by Meyer et al. (1996) and an excellent agreement was found.

4. Results and discussion

4.1. Impact of the osmotic pressure

Osmotic pressure was taken into account in Yang and Vafai (2006) and Ai and Vafai (2006), but not in Chung and Vafai's (2012) work due to its minor influence. Fig. 3 not only shows the impact by using different sets of transport properties as discussed earlier, but also validates the assumption of neglecting osmotic pressure invoked by Chung and Vafai (2012). As can be seen in Fig. 3a, the osmotic pressure has a minor impact on the flow penetration and a negligible effect on the LDL transport, regardless of which set of transport properties is applied. This minor role of the osmotic pressure is due to a dominant hydraulic pressure difference across the arterial wall.

To further investigate the effect of osmotic pressure, its influence is benchmarked against the Darcy resistance in Fig. 3b. The ratio of these two effects is expressed as $-\frac{RT\sigma K}{\mu_{eff}}\frac{\nabla c}{\vec{u}}$ and is displayed across the endothelium and IEL layers, where the osmotic effect is most pronounced (Yang and Vafai, 2006; Ai and Vafai, 2006; Chung and Vafai, 2012). Fig. 3b shows that the osmotic pressure is negligible throughout the endothelium layer by a ratio averaging less than 2% when compared to the Darcy resistance. The osmotic pressure has a larger influence of about 10% to 30%, which still barely affects the overall arterial wall, since more than 90% of hydraulic pressure drop occurs across the endothelium (Yang and Vafai, 2006; Ai and Vafai, 2006; Chung and Vafai, 2012). Therefore one can state osmotic pressure has a negligible effect on the LDL transport within an arterial wall.

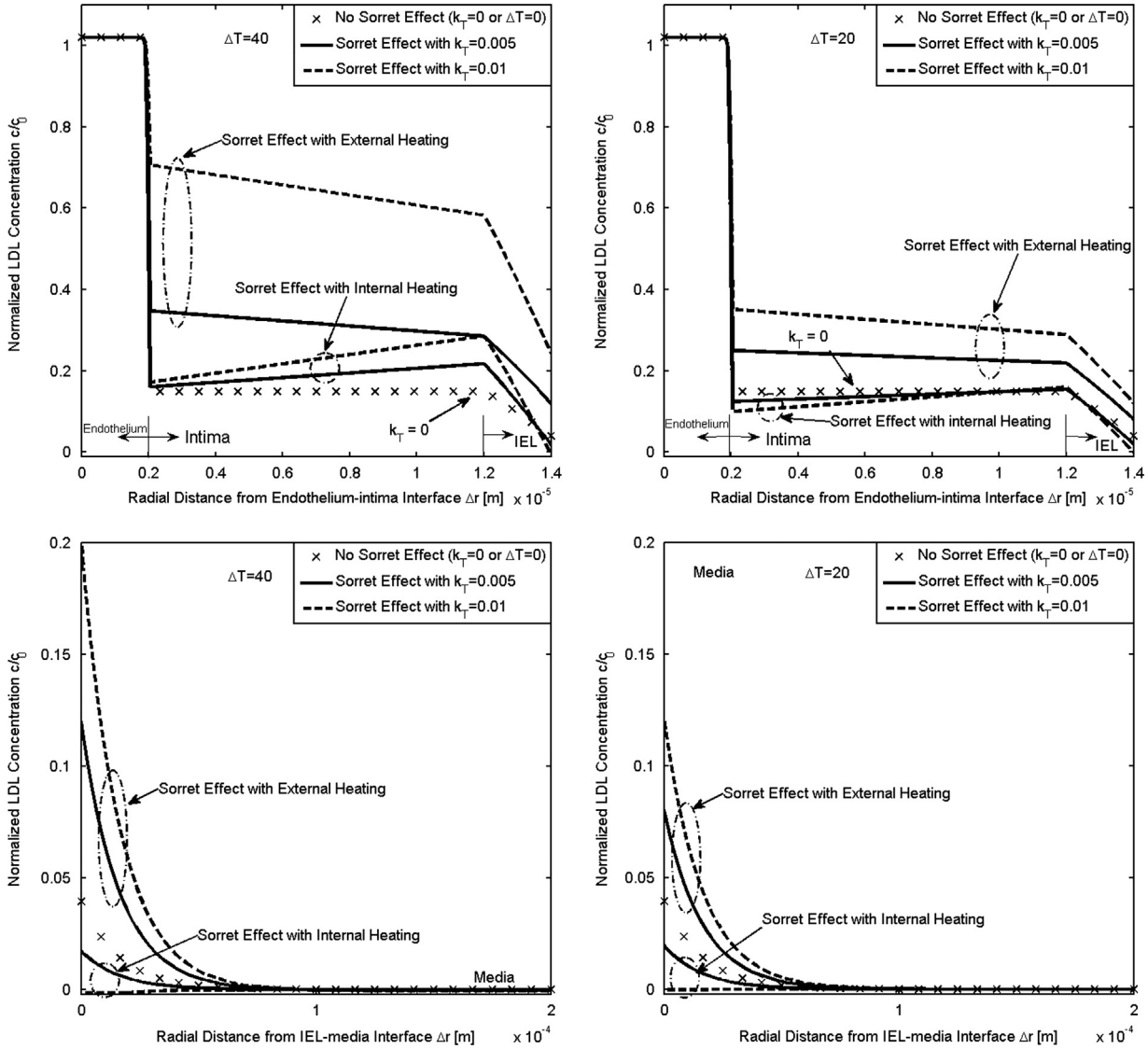

Fig. 5. Soret and hyperthermia effects on the LDL concentration distribution across endothelium, intima, IEL, and media layers.

4.2. Heat transfer model and thermal impact

A thermal model is developed in this study based on the assumption of uniform and homogenous thermal properties (Kolios et al., 1995; Kotte et al., 1996) within the arterial wall. As can be seen in Fig. 2, the temperature-dependent diffusivity has a relatively mild impact within endothelium, intima and IEL (a–c), and a negligible effect within media (d). Influence of variant diffusivity is somewhat more significant within the endothelium and IEL layers due to their overall high transport resistance for the LDL molecular transport. As seen in Fig. 4a, the temperature distribution across the arterial wall shows an almost linear profile due to a very small thermal Peclet number ($\sim 3\times10^{-5}$) and a very thin wall thickness (2×10^{-4} m) as compared to the total radius of artery (3.314×10^{-3} m). Fig. 4a illustrates that the Dufour effect has an insignificant effect on the thermal profile within an arterial wall. The ratio of Dufour flux to the ordinary heat flux shown in Fig. 4b further confirms this point.

4.3. Effect of thermo-diffusion

As seen in Fig. 5, Soret diffusion enhances the LDL transport by increasing the overall LDL concentration within the arterial wall when heat is applied externally. On the other hand, hyperthermia with internal heat can sometimes result in a lower LDL concentration. Soret effect within the endothelium layer is shown to be minor due to dominant convection and diffusion flux (Vafai and Tien, 1989; Vafai and Ettefagh, 1990).

Since Soret diffusion is driven by the temperature gradient, it can be seen that a higher temperature drop across the wall, ΔT, results in a more pronounced Soret flux. Although higher values of k_T enhances Soret effect, a typical value of Soret coefficient k_T is about 0.01

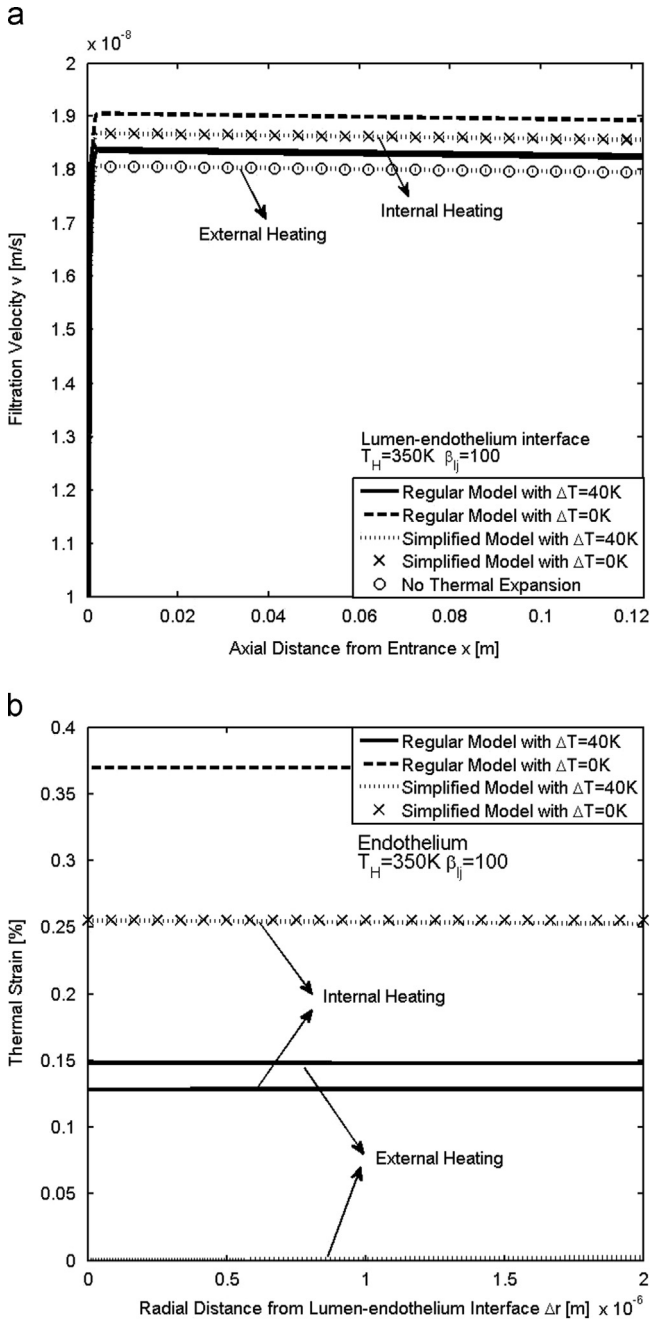

Fig. 6. Effect of thermal expansion on (a) filtration velocity at the lumen-endothelium interface and (b) thermal strain across endothelium.

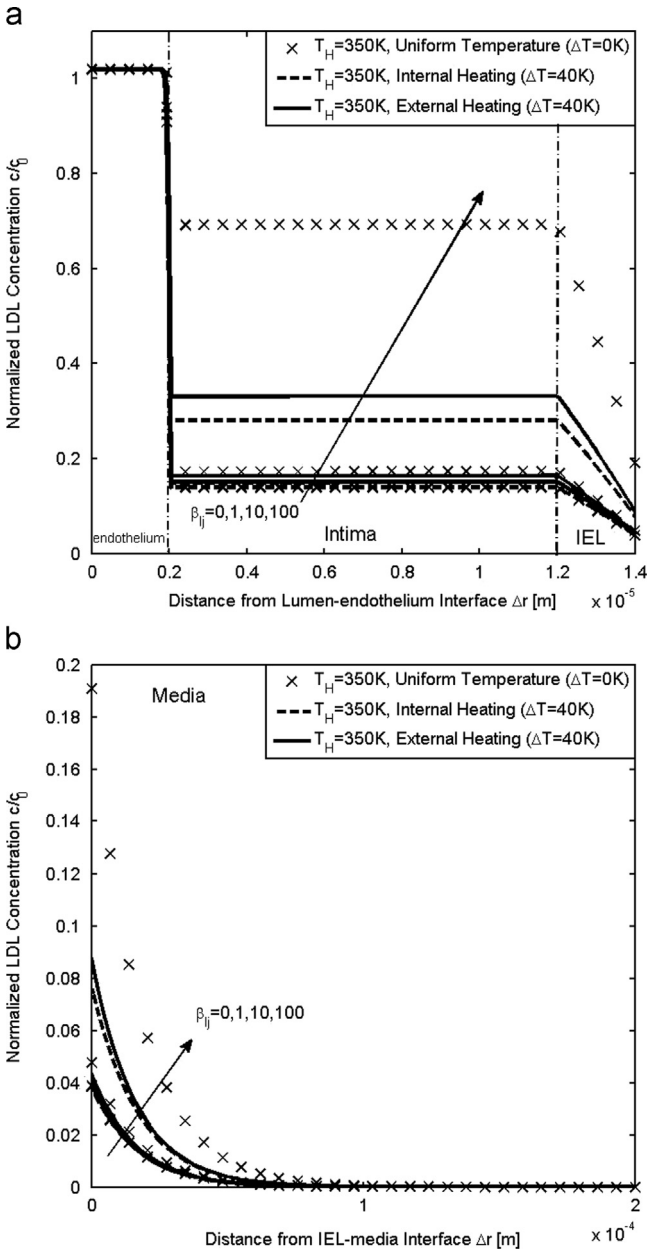

Fig. 7. Effect of temperature drop, ΔT, and leaky-bulk expansion rate, β_{lj} on the LDL concentration distributions across (a) endothelium, intima, IEL, and (b) media ($k_T=0$).

(Chapman and Cowling, 1952; Wakeham et al., 1991) when considering thermo-diffusion. Also, a pronounced Soret effect normally appears with small particles and a less viscous solvent. As such the Soret effect on LDL transport in an artery is expected to be lower ($k_T < 0.01$) due to the heavy mass of LDL molecules, which can still result in a considerable impact compared to osmotic and Dufour effect.

4.4. Effect of thermal expansion

In this part, the thermal expansion and its impact on LDL transport, incorporating temperature-dependent effective LDL diffusivity and Soret effect, is investigated. Based on earlier results, Osmosis and Dufour effect are neglected. The results obtained through both full ($\nabla\sigma_s + f_s = 0$ and $\varepsilon_T = \beta_T(T - T_{ref})$) and simplified ($\varepsilon = \varepsilon_T = \beta_T(T - T_{ref})$) models are compared with those without accounting for thermal expansion and are shown in Fig. 6 for filtration velocity, as well as the strain distribution within the endothelium layer.

Fig. 6a shows that the thermal expansion has a minor enhancement on plasma filtration velocity, which is consistent with the study on the flow induced wall expansion given in Chung and Vafai's (2012) work on fluid–structure interaction. The temperature drop has a significant impact on the wall strain which incorporates the elastic effects. A higher temperature drop will result in a lower average temperature through the wall with a fixed value of T_H, which leads to a smaller thermal expansion. On the other hand, the strain which is based on the simplified model is only affected by the local temperature, irrespective of the temperature drop across the whole arterial wall.

The impact of thermal expansion on LDL concentration across each of the arterial layers is shown in Fig. 7. Applying the full thermal elastic model, the effect of temperature distribution described by different ΔT's as well as the variation of β_{lj}, for both external and internal conditions are illustrated in Fig. 7. Thermal expansion is based on both full and simplified elastic models, incorporating Soret effect with variant k_T. It should be mentioned that variation of thermal-diffusion coefficient, k_T, will have no effect for the $\Delta T = 0$ case because there will be no Soret effect when there is no applied pressure gradient. As seen in Fig. 7, a low temperature differential and a high leaky-bulk expansion rate, β_{lj}, will result in an enhancement via thermal expansion.

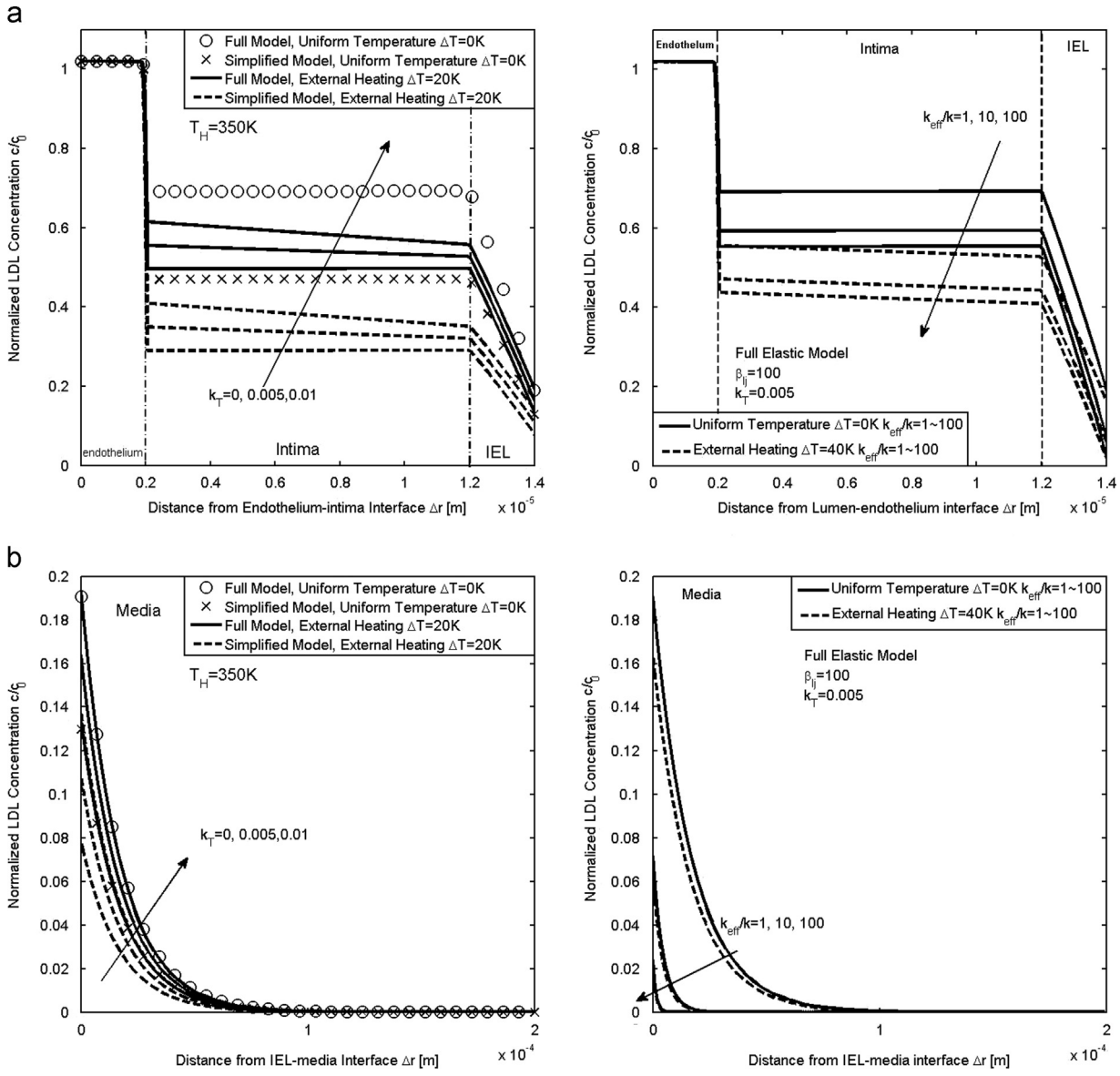

Fig. 8. LDL concentration distribution under thermal expansion incorporating Soret effect with different (a) elastic models and (b) LDL consumption rate$k$ across endothelium, intima, IEL, and media.

A higher temperature differential causes a larger temperature gradient within the layers which will strengthen Soret diffusion of LDL, but this also lowers the overall temperature through the arterial wall and reduces the thermal expansion. This competition between the thermo-diffusion and thermal expansion is dominated by parameters k_T and β_{lj} shown in Fig. 8a. As seen in Fig. 8a, for the full elastic model, as ΔT changes from 0 K to 40 K, the LDL concentration decreases since the reduction of the thermal expansion is more pronounced compared to the enhancement due to the Soret effect, especially for small values of k_T. In contrast, the effect of ΔT on thermal expansion diminishes for the simplified model, so that a larger ΔT results in an increase in LDL concentration due to a stronger Soret diffusion, which is further strengthened for a larger value of k_T.

4.5. Impact of the effective LDL consumption rate

One factor related to the LDL transport that might vary during the hyperthermia process is the LDL consumption rate k which exists within the media layer. The effect of variations in the effective consumption rate on the LDL concentration profiles across each of the arterial layers is illustrated in Fig. 8b. It should be noted that a higher consumption rate leads to a lower LDL concentration.

5. Conclusions

The effect of hyperthermia and coupling attributes on the Low-density lipoprotein (LDL) transport is studied in this work.o, Soret and Dufour effects in an artery for LDL transport are introduced and examined. It is shown that the osmotic and Dufour effects are negligible while the Soret diffusion is shown to have a significant effect in enhancing the LDL transport. The increase in the effective LDL diffusivity and consumption rate due to hyperthermia is shown to have a small effect on the LDL concentration within the arterial wall. It is shown that the thermal expansion enhances LDL transport by causing a larger cross-section area of the leaky junction. The competition between Soret effect and thermal expansion is discussed and quantified. It is established that overall hyperthermia increases the LDL concentration.

Conflict of interest statement

There is no conflict of interest. This manuscript has not been submitted to anywhere else and will not be submitted anywhere else.

References

Ai, L., Vafai, K., 2006. A coupling model for macromolecule transport in a stenosed arterial wall. Int. J. Heat Mass Transfer 49, 1568–1591.

American Heart Association, 2007. Heart Disease and Stroke Statistics—2007 Update. American Heart Association, Dallas.

American Heart Association, 2008. Heart Disease and Stroke Statistics—2008 Update. American Heart Association, Dallas.

Chapman, S., Cowling, T.G., 1952. The Mathematical Theory of Non-Uniform Gases: An Account of the Kinetic Theory of Viscosity, Thermal Conduction, and Diffusion in Gases.

Chung, S., Vafai, K., 2010. Vibration induced mixed convection in an open-ended obstructed cavity. Int. J. Heat Mass Transfer 53, 2703–2714.

Chung, S., Vafai, K., 2012. Effect of the fluid–structure interactions on low-density lipoprotein within a multi-layered arterial wall. J. Biomech. 45, 371–381.

Chung, S., Vafai, K., 2013. Low-density lipoprotein transport within a multi-layered arterial wall—effect of the atherosclerotic plaque/stenosis. J. Biomech. 46, 574–585.

Curry, F.E., 1984a. Mechanics and thermodynamics of transcapillary exchange. Handbook of Physiology, Section 2, The Cardiovascular System, 4. American Physiological Society, Bethesda, MD, pp. 309–374.

Curry, F.E., 1984b. Determinants of capillary permeability: a review of mechanism based on capillary studiesy in the frog. Circ. Res. 59 (4), 367–380.

Fry, D.L., 1985. Mathematical models of arterial transmural transport. Am. J. Physiol. 248, H240–H263.

Gillum, R.F., 1995. Epidemiology of aortic aneurysm in the United States. J. Clin. Epidemiol. 48, 1289–1298.

Hossain, S.S., Hossainy, S.F.A., Bazilevs, Y., Calo, V.M., Hughes, T.J.R., 2011. Mathematical modeling of coupled drug and drug-encapsulated nanoparticle transport in patient-specific coronary artery walls. Comput. Mech. 49 (2), 213–242.

Huang, Y., Weinbaum, S., Rumschitzki, D., Chien, S., 1992. A fiber matrix model for the growth of macromolecular leakage spots in the arterial intima. Adv. Biol. Heat Mass Transfer HTD 231, 81–92.

Huang, Y., Rumschitzki, D., Chien, S., Weinbaum, S., 1994. A fiber matrix model for the growth of macromolecular leakage spots in the arterial intima. J. Biomech. Eng. 116, 430–445.

Hunag, Y., Rumschizki, D., Chien, S., Weinbaum, S., 1997. A fiber matrix model for the filtration through fenestral pores in a compressible arterial intima. Am. J. Physiol. 272, 2023–2039.

Huang, Z.J., Tarbell, J.M., 1997. Numerical simulation of mass transfer in porous media of blood vessel walls. Am. J. Physiol. 273, H464–H477.

Jain, R.K., 1987. Transport of molecules across tumor vasculature. Cancer Metastasis Rev. 6 (4), 559–593.

Jimenez Rios, J.L., Rabin, Y., 2006. Thermal expansion of blood vessels in low cryogenic temperatures Part I: A new experimental device. Cryobiology 52 (2), 269–283.

Karner, G., Perktold, K., Zehentner, H.P., 2001. Computational modeling of macromolecule transport in the arterial wall. Comput. Methods Biomech. Biomed. Eng 4, 491–504.

Katz, M.A., 1985. New formulation of water and macromolecular flux which corrects for non-ideality: theory and derivation, predictions, and experimental results. J. Theor. Biol 112, 369–401.

Kays, W.M., Crawford, M.E., 1993. Convective Heat and Mass Transfer, 1993. McGraw-Hill, New York.

Kedem, O., Katchalsky, A., 1958. Thermodynamic analysis of the permeability of biological membranes to non-electrolytes. Biochem. Biophys. Acta 27, 229–246.

Khakpour, M., Vafai, K., 2008. A comprehensive analytical solution of macromolecular transport within an artery. Int. J. Heat Mass Transfer 51, 2905–2913.

Khanafer, K., Berguer, R., 2009. Fluid–structure interaction analysis of turbulent pulsatileflow within a layered aortic wall as related to aortic dissection. J. Biomech 42, 2642–2648.

Khanafer, K., Bull, J.L., Berguer, R., 2009. Fluid–structure interaction of turbulent pulsatileflow within a flexible wall axisymmetric aortic aneurysm model. Eur. J. Mech. B. Fluids 28, 88–102.

Kolios, M.C., Sherar, M.D., Hunt, J.W., 1995. Large blood vessel cooling in heated tissues: a numerical study. Phys. Med. Biol. 40 (4), 477–494.

Kotte, A., van Leeuwen, G., de Bree, J., van der Koijk, J., Crezee, H., Lagendijk, J., 1996. A description of discrete vessel segments in thermal modelling of tissues. Phys. Med. Biol. 41 (5), 865–884.

Li, J., Stoliarov., S.I., 2013. Measurement of kinetics and thermodynamics of the thermal degradation for non-charring polymers. Combust. Flame 160, 1287–1297.

Liu, X., Fan, Y., Deng, X., 2011. Effect of the endothelial glycocalyx layer on arterial LDL transport under normal and high pressure. J. Theor. Biol. 283 (1, 21), 71–81.

Meyer, G., Merval, R., Tedgui, A., 1996. Effects of pressure-induced stretch and convection on low-density lipoprotein and albumin uptake in the rabbit aortic wall. Circ. Res. 79 (3), 532–540.

Michel, C.C., Curry, F.E., 1999. Microvascular permeability. Physiol. Rev. 79, 703–761.

Moore, J.A., Ethier, C.R., 1997. Oxygen mass transfer calculations in large arteries. J. Biomech. Eng. 119, 469–475.

Prosi, M., Zunino, P., Perktold, K., Quarteroni, A., 2005. Mathematical and numerical models for transfer of low-density lipoproteins through the arterial walls: a new methodology for the model set up with applications to the study of disturbed luminal flow. J. Biomech 38, 903–917.

Rabin, Y., Plitz, J., 2005. Thermal expansion of blood vessels and muscle specimens permeated with DMSO, DP6, and VS55 at cryogenic temperatures. Ann. Biomed. Eng. 33 (9), 1213–1228.

Rappitsch, G., Perktold, K., 1996. Pulsatile albumin transport in large arteries: a numerical simulation study. J. Biomech. Eng. 118, 511–519.

Razi, Y.P., Maliwan, K., Carrier-Mojtabi, M.C., Mojtabi, A., 2005. The Influence of Mechanical Vibrations on Buoyancy Induced Convection in Porous Media, in: Handbook of Porous Media, 321–370.

Shi, W., Vafai, K., 2010. Mixed convection in an obstructed open-ended cavity. Numer. Heat Transfer, Part A 57, 709–729.

Stangeby, D.K., Ethier, C.R., 2002a. Coupled computational analysis of arterial LDL transport—effects of hypertension. Comput. Methods Biomech. Biomed. Eng 5, 233–241.

Stangeby, D.K., Ethier, C.R., 2002b. Computational analysis of coupled blood-wall arterial LDL transport. J. Biomech. Eng. 124, 1–8.

Stoeckel, D., Pelton, A., Duerig, T, 2004. Self-expanding nitinol stents: material and design considerations. Eur. Radiol. 14 (2), 292–301.

Tarbell, J.M., 1993. Bioengineering studies of the endothelial transport barrier. BMES Bull 17, 35–39.

Tarbell, J.M., 2003. Mass transport in arteries and the localization atherosclerosis. Ann. Rev. Biomed. Eng 5, 79–118.

Tada, S., Tarbell, J.M., 2004. Internal elastic lamina affects the distribution of macromolecules in the arterial wall: a computational study. Am. J. Physiol 287, H905–H913.

Tien, C.L., Vafai, K., 1989. Convective and radiative heat transfer in porous media. Adv. Appl. Mech. 27, 225–281.

Vafai, K., Tien, H.C., 1989. A numerical investigation of phase change effects in porous materials. Int. J. Heat Mass Transfer 32, 1261–1277.
Vafai, K., Ettefagh, J., 1990. The effects of sharp corners on buoyancy-driven flows with particular emphasis on outer boundaries. Int. J. Heat Mass Transfer 33, 2311–2328.
Vafai, K., Hadim, H., 2000. Overview of current computational studies of heat transfer in porous media and their applications—natural convection and mixed convection. Advances in Numerical Heat Transfer, vol. 2. Taylor & Francis, New York, pp. 331–371.
Wada, S., Karino, T., 2000. Computational study on LDL transfer from flowing blood to arterial walls. In: Yamaguchi, T. (Ed.), Clinical Applications of Computational Mechanics to the Cardiovascular System. Springer, Berlin, pp. 157–173.
Wakeham, W.A., Nagashima, A., Sengers, J.V., 1991. Experimental Thermodynamics, vol. III. Blackwell Scientific Publications, Oxford.
Weinbaum, S., Tsay, R., Curry, F.E., 1992. A three-dimensional junction-pore-matrix model for capillary permeability. Microvasc. Res. 44, 85–111.
Yang, N., Vafai, K., 2006. Modeling of low-density lipoprotein (LDL) transport in the artery—effects of hypertension. J. Int. Heat Mass Transfer 49, 850–867.
Yang, N., Vafai, K., 2008. Low-density lipoprotein (LDL) transport in an artery—a simplified analytical solution. J. Int. Heat Mass Transfer 51, 497–505.
Yuan, F., Chien, S., Weinbaum, S., 1991. A new view of convective–diffusive transport processes in the arterial intima. J. Biomech. Eng. 133, 314–329.